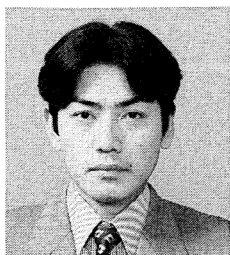


**MODELING OF PH PROFILE IN PORE WATER
BASED ON MASS TRANSPORT AND CHEMICAL EQUILIBRIUM THEORY**

(Translation from Proceedings of JSCE, No.648/V-47, May 2000)



Tetsuya ISHIDA



Koichi MAEKAWA

The authors present a computational system that can deal with pH fluctuations and the decomposition of cementitious materials exposed to various environmental actions. In order to evaluate the fall in pH due to carbon dioxide, material models are developed for the transport and equilibrium of carbon dioxide, ionization, ion equilibriums, and the carbonation reaction based on thermo-dynamic theory. The material properties of concrete are evaluated by considering the inter-relationships among hydration, moisture transport, and pore-structure development based on fundamental physical material models. The proposed system is able to reasonably predict the carbonation phenomena and pH profiles in concrete for arbitrary conditions.

Keywords: *Durability, pH, mass transport, chemical equilibrium, carbonation, pore solution*

Tetsuya Ishida is a research associate in the Department of Civil Engineering at University of Tokyo, Japan. He obtained his D.Eng from University of Tokyo in 1999. His research interests cover mass/energy transport phenomena in concrete, durability design, and the mechanisms of shrinkage and creep of concrete. He is a member of the JSCE and the JCI.

Koichi Maekawa serves as professor in the Department of Civil Engineering at the University of Tokyo, Japan. He obtained his D.Eng. from University of Tokyo in 1985. He specializes in nonlinear mechanics and constitutive laws of reinforced concrete, seismic analysis of structures, and concrete thermodynamics. He is a member of the JSCE and the JCI.

1. INTRODUCTION

It is a well-known fact that steel corrosion reduces the serviceability and safety performance of a reinforced concrete structure. Usually, concrete maintains very alkaline conditions, which leads to a passive layer forming on the steel surface. However, several types of environmental action, including action by carbonic, sulphuric, and nitric acid, can cause the pH value of concrete pore water to decrease. Under low-pH conditions, the passive layer around the steel surface breaks down, and rust readily appears on the surface. In order to evaluate performance factors of a concrete structure in a corrosive environment, it is therefore essential to quantify the neutralization of concrete, that is to say, the pH reduction due to such environmental acids. In this research, the authors mainly focus on the carbonation phenomenon, and aim to predict pH fluctuations and material degradations under carbonic acid attack.

Gaseous carbon dioxide readily dissolves into the pore water of concrete, and it turns into a carbonic acid solution. Carbonic ions dissociate from the carbonic acid solution releasing protons, which then react with calcium ions to form calcium carbonate. In this reaction, carbonic acid neutralizes alkalis in the pore water, mainly consuming calcium hydroxide whose solubility is the highest in cement hydrates. As a result, as the calcium hydroxide is consumed, the pH value drops. From a thermodynamic point of view, the carbonation reaction is sure to progress under the condition that carbon dioxide exists, since the free energy of calcium carbonate is lower than that of calcium hydroxide [1].

In the conventional approach to studying the carbonation phenomenon, empirical formulae are generally used for its prediction. Many such formulae were formulated based on the assumption that carbonation would progress in proportional to exposure time as [1][2],

$$X_c = b\sqrt{t} \quad (1)$$

where, X_c : depth of carbonation, b : carbonation rate coefficient, and t : exposure time. In fact, depth of carbonation X_c can be obtained by solving a linear diffusion equation for CO_2 gas. Namely, the above equation involves the assumption that the depth of carbonation is associated with the amount of carbon dioxide diffusing through the concrete materials. In these methods, the carbonation rate coefficient b is empirically determined as a function of water-to-cement ratio, strength, and environmental conditions [3][4][5][6].

Recently, several studies have evaluated the carbonation process using a microphysical-based approach [7][8][9][10]. In these studies, diffusion processes in concrete (moisture, carbon dioxide, and so on) and the carbonation process are modeled, and a linear or a non-linear diffusion equation is solved in the analysis. Depth of carbonation is evaluated by the amount of remaining calcium hydroxide and/or produced calcium carbonate in the concrete. Some of them also aim to solve ion equilibriums and evaluate the pH value of pore water [11][12].

In this study, we introduce a generalized computational method that can deal with pH fluctuations of pore water and degradation of the microstructure due to carbonation for arbitrary initial and environmental conditions. To simulate carbonation phenomena in concrete, the equilibrium between gaseous and dissolved carbon dioxide, their transports, ionic equilibriums, and the carbonation reaction process are formulated based on thermodynamics and chemical equilibrium theory. Material properties of the concrete, which are necessary for computation of the above formulations, are evaluated considering the inter-relationships among hydration, moisture transport, and pore-structure development processes based on fundamental physical material models. By means of this methodology, the proposed system can be applied not only to the carbonation phenomenon, but also to prediction of the pH profile in pore solutions attacked by other acids, such as sulphuric acid, nitric acid, and so on.

This paper aims at the carbonation process under an isothermal environment (25°C), and the

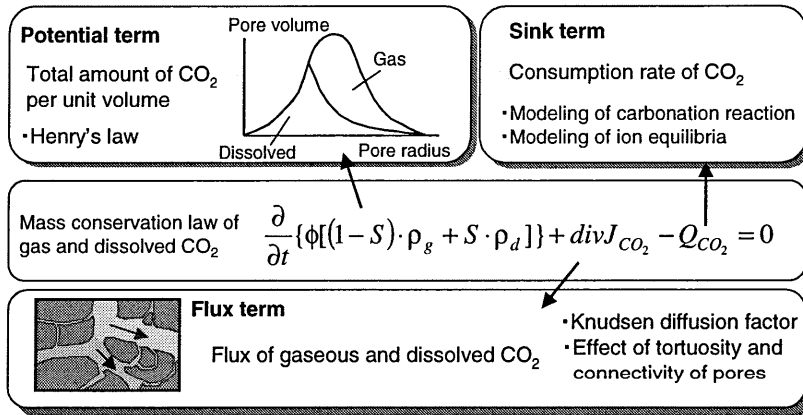


Fig.1 Governing equation and constituting models

modeling for arbitrary temperature remains for future study. Therefore, in implementing the model, the unique values are given to Henry's constant describing CO₂ equilibrium, reaction rate coefficient of carbonation, equilibrium constants of ionic concentration, and solubility.

2. Modeling of carbon dioxide transport and equilibrium

2.1 Mass conservation law for carbon dioxide

In general, when dealing with mass, energy and momentum flows in a control volume, the starting point is to build appropriate balance equations. In other words, the summation of rate of mass efflux from a control volume, the rate of mass flow into the control volume, and the rate of accumulation of mass within the control volume should be zero. In this section, the mass balance conditions for carbon dioxide in a porous medium are formulated. Two phases of carbon dioxide existing in concrete are considered; gaseous carbon dioxide and carbon dioxide dissolved in pore water. By solving the mass balance equation under given initial and boundary conditions, the non-steady state conduction of carbon dioxide is quantified. The mass balance equation for a porous medium can be expressed as (Fig.1),

$$\frac{\partial}{\partial t} \{ \phi [(1-S) \cdot \rho_g + S \cdot \rho_d] \} + \text{div} J_{CO_2} - Q_{CO_2} = 0 \quad (2)$$

where, ϕ : porosity, S : saturation of porosity, ρ_g : density of gaseous carbon dioxide [kg/m³], ρ_d : density of dissolved carbon dioxide in pore water [kg/m³], and J_{CO_2} : total flux of dissolved and gaseous carbon dioxide [kg/m².s]. The first term in eq.(2) represents the rate of change in total amount of carbon dioxide per unit time and volume, the second term is the flux of carbon dioxide, and the third term Q_{CO_2} is a sink term. The above equation gives the concentrations of gaseous and dissolved carbon dioxide with time and space.

The above conservation law must be satisfied in all material systems and so it applies to the field of concrete materials. In the following chapters, each term will be modeled based on the specific characteristics of concrete materials, i.e., the equilibrium and transport of gaseous and dissolved CO₂, and the consumption rate of carbon dioxide.

2.2 Equilibrium conditions for gaseous and dissolved carbon dioxide

The local equilibrium between gaseous and dissolved carbon dioxide is represented here by Henry's law, which states the relationship between gas solubility in pore water and the partial gas pressure. In this research, we assume that the system will instantaneously reach local equilibrium

between the two phases as [15],

$$P_{CO_2} = H'_{CO_2} \cdot \rho'_d \quad (3)$$

where, P_{CO_2} : equilibrium partial pressure of carbon dioxide in the gas phase, ρ'_d : mole fraction of gaseous CO_2 [mol of CO_2 /total mol of solution], and H'_{CO_2} : Henry's constant for carbon dioxide ($=1.45 \times 10^8$ [Pa/mol fraction] at 25 degrees Celsius). For one cubic meter of dilute solution, the moles of water in the solution n_{H_2O} will be approximately 5.56×10^4 [mol/m³]; accordingly the concentration of dissolved carbon dioxide per cubic meter of solution ρ_d [kg/m³] can be expressed as,

$$\rho_d = \frac{P_{CO_2}}{H'_{CO_2}} \cdot n_{H_2O} \cdot M_{CO_2} = \frac{P_{CO_2}}{H_{CO_2}} \quad (4)$$

where, M_{CO_2} is the molecular mass of carbon dioxide ($=0.044$ [kg/mol]). The complete perfect-gas equation is then,

$$P_{CO_2} = \frac{\rho_g RT}{M_{CO_2}} \quad (5)$$

where, ρ_g : concentration of gaseous carbon dioxide [kg/m³], R : gas constant [J/mol.K], and T : temperature [K]. From eqs. (4) and (5), the equilibrium relationship between gas and dissolved CO_2 can be expressed as,

$$\rho_g = \frac{M_{CO_2}}{RT} \cdot H_{CO_2} \cdot \rho_d = K_{CO_2} \cdot \rho_d \quad (6)$$

After dissolving into solution, carbon dioxide reacts with calcium ions, and so the concentration of dissolved CO_2 can fluctuate from the above equilibrium condition. Strictly speaking, therefore, the equilibrium condition cannot be formulated by Henry's law alone; it is also necessary to determine the amount of dissolved CO_2 based on the rate of chemical reactions, which represents kinetic fluctuations dependent on the distribution of CO_2 concentration. However, it seems difficult to take into account such kinetic fluctuations as it is, and in fact, it is expected that the rate of CO_2 gas dissolution will be faster when the partial pressure of CO_2 gas becomes large. For these reasons, in our model we assume that the amount of dissolved CO_2 can be approximately described by Henry's law [7][8].

2.3 Modeling of carbon dioxide transport

Transport of CO_2 is considered for both dissolved and gaseous carbon dioxide phases. The CO_2 gas can move through unsaturated pores, whereas dissolved CO_2 is transported within pore liquid water. In the model, it is assumed that all pores have a cylindrical shape.

Diffusion in a porous body may occur by one or more of three mechanisms: molecular diffusion (Fick diffusion), Knudsen diffusion, and surface diffusion. In the model, molecular diffusion and Knudsen diffusion are considered, whereas the contribution of surface diffusion is ignored, since surface diffusion takes places when molecules which have been adsorbed are transported along the pore wall, and normally it plays a minor role in diffusion within concrete materials under typical environmental conditions [13][16][17].

As the relative humidity in a pore decreases, the porous medium for gas transport becomes finer. If the pores through which the gas is traveling are quite small, the molecules will collide with the

walls more frequently than with each other. This is known as Knudsen diffusion. The conditions transiting to Knudsen diffusion are expressed by the following equation using Knudsen number N_k as,

$$N_k = \frac{l_m}{2r_e} > 1.0 \quad (7)$$

where, l_m : the mean free path length of a molecule of gas, and r_e : the actual pore radius, which means the radius of a pore minus the thickness of the adsorbed layer of water obtained by B.E.T. theory [13]. Considering both molecular diffusion and Knudsen diffusion, the one dimensional gaseous flux through a single pore of radius r can be expressed as,

$$J_g^r = -\frac{D_0^g}{1 + (l_m/2r_e)} \frac{\partial \rho_g}{\partial x} \quad (8)$$

where, D_0^g [m^2/s] is the diffusivity of CO_2 in a free atmosphere ($=1.34 \times 10^{-5}$) [15]. Similarly, the flux of dissolved carbon dioxide can be obtained as,

$$J_d^r = -D_0^d \frac{\partial \rho_d}{\partial x} \quad (9)$$

where, D_0^d [m^2/s] is the diffusivity of dissolved CO_2 in pore water ($=1.0 \times 10^{-9}$) [15].

The total flux within porous bodies can be obtained by integrating eqs. (8) and (9) over the entire porosity distribution. For example, let us consider the equilibrium condition of moisture during a monotonic wetting phase, in which there is no inkbottle effect [21]. In this case, based on the thermodynamic conditions, a certain group of pores whose radii is smaller than the specific radius r_c at which a liquid-vapor interface forms are completely filled with water, whereas larger pores remain empty or partially saturated so that these pores can be routes for the transfer of CO_2 gas. Therefore, by integrating the gaseous and dissolved fluxes of CO_2 , respectively, the entire flux of carbon dioxide is formulated as,

$$J_{\text{CO}_2} = -\left(\frac{\phi D_0^d}{\Omega} \int_0^{r_c} dV \frac{\partial \rho_d}{\partial x} + \frac{\phi D_0^g}{\Omega} \int_{r_c}^{\infty} \frac{dV}{1 + N_k} \frac{\partial \rho_g}{\partial x} \right) \quad (10)$$

where, V is the pore volume, and $\Omega = (\pi/2)^2$ accounts for the average tortuosity of a single pore as a fictitious pipe for mass transfer. The latter parameter considers the tortuosity of a hardened cement paste matrix, which is uniformly and randomly connected in a 3-D system [13]. The first term of the right-hand side in equation (10) denotes the diffusive component of dissolved carbon dioxide in the pore liquid, whereas the second term represents the component of gaseous diffusion. The substitution of porosity saturation S for the integrals in the above equation in order to generalize the expression for an arbitrary moisture history gives,

$$J_{\text{CO}_2} = -(D_{d\text{CO}_2} \nabla \rho_d + D_{g\text{CO}_2} \nabla \rho_g) = -(D_{d\text{CO}_2} + D_{g\text{CO}_2} \cdot K_{\text{CO}_2}) \nabla \rho_d \quad (11)$$

$$D_{d\text{CO}_2} = \frac{\phi S}{\Omega} D_0^d \quad D_{g\text{CO}_2} = \frac{\phi \cdot D_0^g}{\Omega} \frac{(1-S)}{1 + l_m/2(r_m - t_m)} \quad (12)$$

where, $D_{g\text{CO}_2}$: diffusion coefficient of gaseous CO_2 in a porous medium [m^2/s], and $D_{d\text{CO}_2}$: diffusion coefficient of dissolved CO_2 in a porous medium [m^2/s]. In eq. (12), the integral of the Knudsen number is simplified so that it can be easily put into practical computational use; r_m is the average radius of unsaturated pores, and t_m is the thickness of the adsorbed water layer in the

pore whose radius is r_m .

It has to be noted that the above formulations do not include the complete effects of the connectivity of pores on diffusivity. That is to say, considering one-dimensional transport of gaseous phases, all unsaturated pores, which are route for gas movement, are assumed to be connected with perfect continuity (Fig.2, left). In actual pore structures that have complicated connectivity, however, the movement of gas will be blocked by saturated pores containing liquid water (Fig.2, right). Here, as the saturation of pores decreases, the open pore space gains higher connectivity so that total diffusivity increases nonlinearly. One potential model for this phenomenon would be based on percolation theory [14], however, we adopt the following model for the sake of simplicity.

Let us consider a finite field that consists of segments small enough to have continuity of pores, as shown in Fig.2, right. In the cross section of each unit, the ratio of gas transportation paths will be $(1-S)$. If we assume that the probability of unsaturated pores being connected to each other would be proportional to the ratio of the volume in a cross section, the overall flux can be expressed as,

$$D_{gCO_2} = \frac{\phi \cdot D_0^g}{\Omega} \frac{(1-S)^n}{1 + l_m/2(r_m - t_m)} \quad D_{dCO_2} = \frac{\phi S^n}{\Omega} D_0^d \quad (13)$$

where, n is a parameter representing the connectivity of the pore structure, and might vary with the geometrical characteristics of the pores. However, at this stage, it is difficult to take account of the exact connectivity situation. In this study, through sensitivity analysis, n is tentatively assumed to be 4.0, which is the most appropriate value for expressing the reduction of CO_2 diffusivity with the decrease of relative humidity (Fig.3).

In order to evaluate the hysteresis behavior of moisture saturation during drying-wetting cycles, the authors have developed a moisture isotherm model that considers the connectivity of pores with two different radii [21]. The above expression of saturation S involves the blockage effect due to the connection of pores in its simplest form. However, the connectivity factor considered in the moisture isotherm model cannot alone evaluate the non-linear behavior in CO_2 diffusion process with relative humidity change. This might be because of the difference between the characteristics of CO_2 gas transport and moisture transport; in the case of moisture transfer, the local equilibrium between liquid and vapor is maintained, and the movement of the vapor phase is dominant, whereas the diffusive movement of CO_2 gas is completely blocked by the existence of pore water.

Figure 3 compares the CO_2 diffusivity calculated by the model and by an empirical formula obtained by diffusion tests [18]. It can be seen that the non-linear behavior of CO_2 diffusivity is reasonably well predicted.

3. Modeling of carbonation reaction

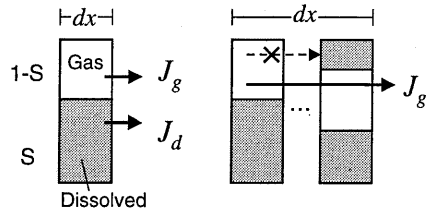


Fig.2 Effect of connectivity of pores on CO_2 transport

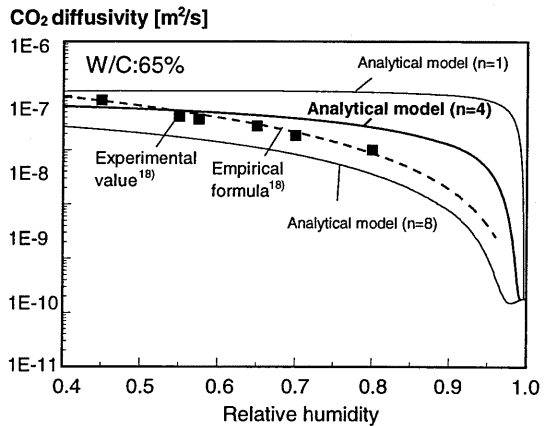


Fig.3 Relationship between CO_2 diffusivity and relative humidity

3.1 Formulation of carbonation reaction rate

The carbonation phenomenon in cementitious materials is simply described by the following equation of ionic reaction.



Calcium ions resulting from the dissolution of calcium hydroxide are assumed to react with carbonate ions, whereas the reaction of silicic acid calcium hydrate (C-S-H) is not considered. This is based on the fact that the solubility of C-S-H is quite low compared with that of calcium hydroxide, i.e., the solubility of C-S-H (in the case of $6\text{CaO}\cdot 5\text{SiO}_2\cdot 6\text{H}_2\text{O}$) $K_{sp} = [\text{Ca}^{2+}]^6[\text{HSiO}_3^-]^5[\text{OH}^-]^7 = 5.5 \times 10^{-49}$, and the solubility of $\text{Ca}(\text{OH})_2$ $K_{sp} = [\text{Ca}^{2+}][\text{CO}_3^{2-}] = 4.14 \times 10^{-5}$ [1]. It has to be noted, however, that these values are for a normal environment. Therefore, we understand that it is necessary to consider chemical reactions of C-S-H solution for the sake of predicting deterioration phenomena under severe environmental action and/or environmental action over quite a long time.

The rate of the reaction in eq.(14) can be expressed by the following differential equation, assuming that the reaction is of the first order with respect to Ca^{2+} and CO_3^{2-} concentrations as,

$$Q_{\text{CO}_2} = \frac{\partial(C_{\text{CaCO}_3})}{\partial t} = k[\text{Ca}^{2+}][\text{CO}_3^{2-}] \quad (15)$$

where, C_{CaCO_3} : concentration of calcium carbonate [mol/l], and k : reaction rate coefficient [l/mol.sec]. The concentration of calcium carbonate per unit time obtained by the above equation is equal to the consumption rate of carbonic acid, which is the sink term Q_{CO_2} in the mass balance equation (2).

As already mentioned, eq. (15) is a differential equation determining the reaction rate of calcium ions and carbonate ions in solution. For this reaction to occur, molecular collisions of each ion are necessary, and the right-hand side of eq. (15) represents the rate of such collisions. Here, a molecular decomposition occurs to form a new product only if a molecule has an energy more than the activation energy. The ratio of molecules having a kinetic energy above this activation energy is determined by the Boltzmann distribution law, which shows strong dependency on temperature. In the above equation, therefore, a temperature effect is involved in the reaction rate coefficient k . In other words, k only represents the reaction rate at a certain temperature. Therefore, in order to evaluate the carbonation process at an arbitrary temperature, it is necessary to consider the temperature effect on rate reaction coefficient k . Still, in this paper, a unique coefficient is applied, i.e., coefficient k is assumed to be constant ($k=2.08$ [l/mol.sec]) using a value determined from several sensitivity analyses. The authors understand that modeling of the carbonation rate is desired in the future, using Arrhenius's law of chemical reaction.

The above discussion concludes the formulation of the carbonation reaction. In the following chapter, we will describe the modeling of the ionic equilibrium in order to obtain the reaction rate by from eq. (15).

3.2 Ion equilibria in solution

In the pore solutions of concrete, various ions coexist; calcium, aluminum, iron, magnesium, sodium, potassium, and others. Though sodium and potassium ions form carbonate salts, here we consider only calcium ions, which are comparatively abundant (in case of ordinary cement, CaO: 65%, Na₂O: 0.3%, K₂O: 0.5%). It has been reported, however, that sodium and potassium ions may cause pH fluctuations, and also a change in the carbonation rate [19]. In addition, it has been

also pointed out that the pH value after carbonation would depend on the concentrations of these ions [12]. Therefore, in order to accurately evaluate the pH profile, it would be necessary to consider these alkali ions as well as calcium ions. As a first approximation, however, we consider only calcium ions, and other ions will be considered in a future study.

The dissociations of the ions considered in the model are shown by the following eq. (16). We consider the dissociation of water and carbonic acid, and the dissolution and dissociation of calcium hydroxide and calcium carbonate.

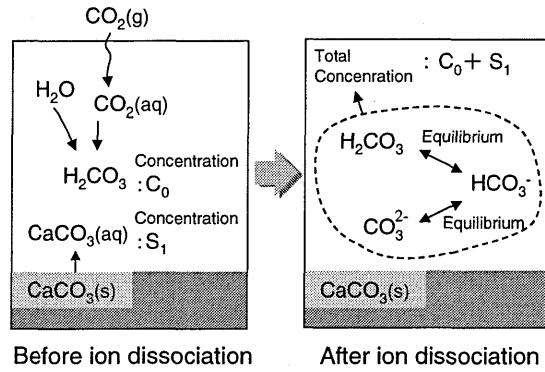
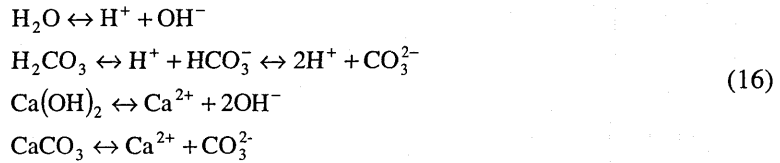


Fig.4 Mass balance and equilibrium conditions for carbonic acid



Strictly speaking, the representation of a proton by H^+ might not be correct. Rather, the hydronium ion H_3O^+ is present in water and confers acidic properties on aqueous solutions. However, it is customary to use the symbol H^+ in place of H_3O^+ , so H^+ will be used in the following discussion.

As shown in eq.(16), carbonation is an acid-base reaction, where cations and anions act as a Brönsted acid and base, respectively. Furthermore, the solubility of precipitations is dependent on the pH of the pore solution. Therefore, in order to obtain each ionic concentration at an arbitrary stage, the authors firstly introduce an equation with respect to the concentration of protons $[\text{H}^+]$. Once the concentration of protons $[\text{H}^+]$ is known, each equilibrium condition can be calculated for a given pH value. For each ion, the following basic principles should be satisfied [20]:

1. Law of mass action
2. Mass conservation law
3. Proton balance

First of all, let us consider the equilibrium reaction of carbonic acid. Based on the law of mass action, the corresponding equilibrium expressions should be satisfied as,

$$K_w = [\text{H}^+][\text{OH}^-] \quad K_a = \frac{[\text{H}^+][\text{HCO}_3^-]}{[\text{H}_2\text{CO}_3]} \quad K_b = \frac{[\text{H}^+][\text{CO}_3^{2-}]}{[\text{HCO}_3^-]} \tag{17}$$

where, K_i is the equilibrium constant of concentration for each dissociation. We give these values as $K_w=1.00 \times 10^{-14}$, $K_a=1.00 \times 10^{-14}$, and $K_b=4.79 \times 10^{-14}$ at 25°C respectively.

Next, the mass conservation law is applied for the ions resulting from the dissolution of carbon dioxide and re-dissolution of calcium carbonate as (Fig.4),

$$C_0 + S_1 = [\text{H}_2\text{CO}_3] + [\text{HCO}_3^-] + [\text{CO}_3^{2-}] \tag{18}$$

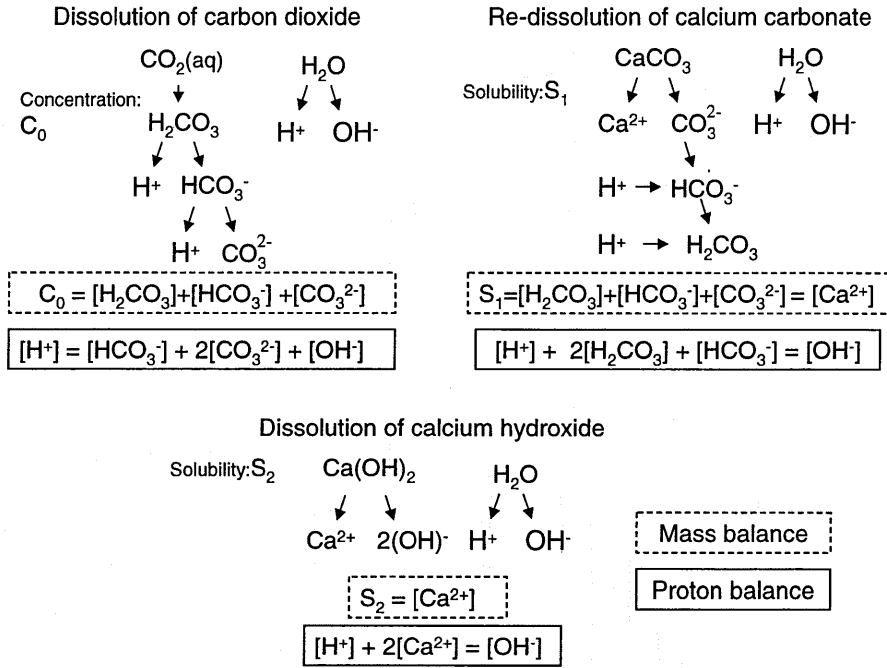


Fig.5 Mass and proton balance equations in each system

where, C_0 is the concentration of dissolved carbon dioxide [mol/l], which can be obtained from p_d in eq.(2). S_1 is the solubility of calcium carbonate, which can be calculated using the solubility-product constant discussed later.

Using eqs.(17) and (18), concentrations of H_2CO_3 , HCO_3^- and CO_3^{2-} can be obtained as,

$$\begin{aligned}
 [H_2CO_3] &= \alpha_0 \cdot (C_0 + S_1) & \alpha_0 &= \frac{[H^+]^2}{[H^+]^2 + K_a[H^+] + K_a K_b} \\
 [HCO_3^-] &= \alpha_1 \cdot (C_0 + S_1) & \alpha_1 &= \frac{K_a[H^+]}{[H^+]^2 + K_a[H^+] + K_a K_b} \\
 [CO_3^{2-}] &= \alpha_2 \cdot (C_0 + S_1) & \alpha_2 &= \frac{K_a K_b}{[H^+]^2 + K_a[H^+] + K_a K_b}
 \end{aligned} \tag{19}$$

As this shows, the concentrations of H_2CO_3 , HCO_3^- and CO_3^{2-} are functions of S_1 . It is therefore necessary to obtain the solubility of calcium carbonate. That solubility can be derived by the following relationship as,

$$K_{sp}^1 = [Ca^{2+}][CO_3^{2-}] \tag{20}$$

where, K_{sp}^1 is the solubility-product constant of the calcium carbonate ($=4.7 \times 10^{-9}$, at 25°C) [20]. Similarly, the solubility of calcium hydroxide can be calculated as,

$$K_{sp}^2 = [Ca^{2+}][OH^-]^2 \tag{21}$$

where, K_{sp}^2 is the solubility-product constant of the calcium hydroxide ($=5.5 \times 10^{-6}$, at 25°C) [20].

In looking at the ion dissociations shown in eqs. (20) and (21), it is necessary to consider the common ion effect on the solubility. Namely, carbonate ions in eq. (20) come not only from the decomposition of calcium carbonate, but also from that of carbonic acid. As for the calcium ions in eqs. (20) and (21), a similar effect should be considered here as well. Considering these common ion effects on each solubility, the solubility of calcium carbonate S_1 and that of calcium hydroxide S_2 can be substituted in eqs. (19), (20) and (21) as,

$$K_{sp}^1 = (S_1 + S_2) \cdot \alpha_2 (C_0 + S_1) \quad (22)$$

$$K_{sp}^2 = (S_1 + S_2) \cdot [\text{OH}^-]^2 \quad (23)$$

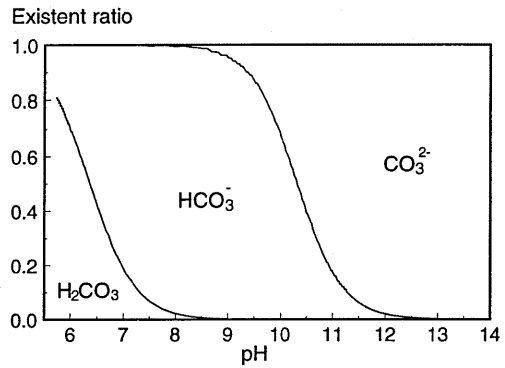


Fig.6 Relationship between equilibrium of carbonic acid and pH in solution

Next, the law of mass balance is considered. Figure 5 shows the mass balance conditions in each system: dissolution of carbon dioxide, re-dissolution of calcium carbonate, and dissolution of calcium hydroxide. In order to distinguish the sources of ion dissociation, concentrations of ions are expressed with suitable notation, that is, $[i]_d$, $[i]_s$, and $[i]_c$ are the concentrations of ions dissociated from the dissolution of CO_2 gas, calcium carbonate and calcium hydroxide, respectively. For example, the total concentration of carbonic acid $[\text{H}_2\text{CO}_3]$ shown in eq. (9) becomes the summation of $[\text{H}_2\text{CO}_3]_d$ from CO_2 gas and $[\text{H}_2\text{CO}_3]_s$ from CaCO_3 .

From the mass conservation conditions before and after ion dissociation, the following equations should be satisfied:

$$C_0 = [\text{H}_2\text{CO}_3]_d + [\text{HCO}_3^-]_d + [\text{CO}_3^{2-}]_d \quad (24)$$

$$S_1 = [\text{H}_2\text{CO}_3]_s + [\text{HCO}_3^-]_s + [\text{CO}_3^{2-}]_s = [\text{Ca}^{2+}]_s \quad (25)$$

$$S_2 = [\text{Ca}^{2+}]_c \quad (26)$$

In addition, the above ions should satisfy the law of proton balance, in which the amount of donors is equal to that of accepters in terms of protons in the Brönsted-Lowry theory. The equation deduced by this law of proton balance is also shown in Fig.5. The overall proton balance equation can be obtained by the summing up each equation as,

$$[\text{H}^+] + 2[\text{Ca}^{2+}]_c + 2[\text{H}_2\text{CO}_3]_s + [\text{HCO}_3^-]_s = [\text{OH}^-] + [\text{HCO}_3^-]_c + 2[\text{CO}_3^{2-}]_c \quad (27)$$

From the above equations describing ion equilibrium conditions, we finally obtain,

$$[\text{H}^+] + 2S_2 + 2S_1\alpha_0 + S_1\alpha_1 = \frac{K_w}{[\text{H}^+]} + \alpha_1 C_0 + 2\alpha_2 C_0 \quad (28)$$

Equation (28) shows that the concentration of protons $[\text{H}^+]$ can be obtained at an arbitrary stage as an exact solution, given the concentrations of calcium hydroxide and carbonic acid before dissociation. After the concentration of protons is known, each individual ionic concentration can be calculated. As an example of a computation using the proposed method, the relationship between the pH value in solution and the existent ratio of carbonic acid, carbonic hydroxide ion, and carbonate ion is shown in Fig.6. In the high pH range, carbonic ions are dominant, whereas carbonic hydroxide ions increase under low pH conditions.

3.3 Change of pore structure due to carbonation

It has been reported that the micro-pore structure of cementitious materials may change due to carbonation [1]. In general, pore structures are thought to become finer with carbonation. However, there is no consensus on how porosity and porosity distribution will change. For example, one report has noted that only the porosity of specific radii will decrease, whereas another concluded that porosity will decrease but the porosity distribution will not change at all.

In this research, we consider changes in porosity with carbonation using a simplified model. We assume that the porosity distribution does not change, but that porosity decreases as carbonation progresses. Regarding the quantitative evaluation of this change, an empirical set of equations proposed in past research is modified and used [7]:

$$\begin{aligned} \phi' &= \phi(R_{\text{Ca(OH)}_2}) & 0.6 < R_{\text{Ca(OH)}_2} < 1.0 \\ \phi' &= 0.5 \cdot \phi & R_{\text{Ca(OH)}_2} \leq 0.6 \end{aligned} \quad (29)$$

where, ϕ : porosity before carbonation, ϕ' : porosity after carbonation, and $R_{\text{Ca(OH)}_2}$: ratio of the amount of consumed Ca(OH)_2 to the total amount of Ca(OH)_2 .

Theoretically, a finer porosity results from the volume change of hydrates due to carbonation; the crystal volume of calcium carbonate is approximately 11.7 percent more than that of calcium hydroxide. The authors understand that it would be possible to establish a more generalized treatment by implementing this volume change into the micro-pore structure model [13], but this enhancement remains for future study.

4. Verifications and numerical simulations

4.1 Thermo-hygro system DuCOM

The formulations described thus far were implemented into the finite-element computational program DuCOM. The overall computational scheme is shown in Fig.7. The constituent material models are based on microphysical phenomena such as hydration, moisture transport, and the formation of pore-structure, and they take into account the inter-relationships between these in a natural way. A detailed discussion of the material models and system dynamics for describing their interactions can be found in published papers [13][21][22][23] [24].

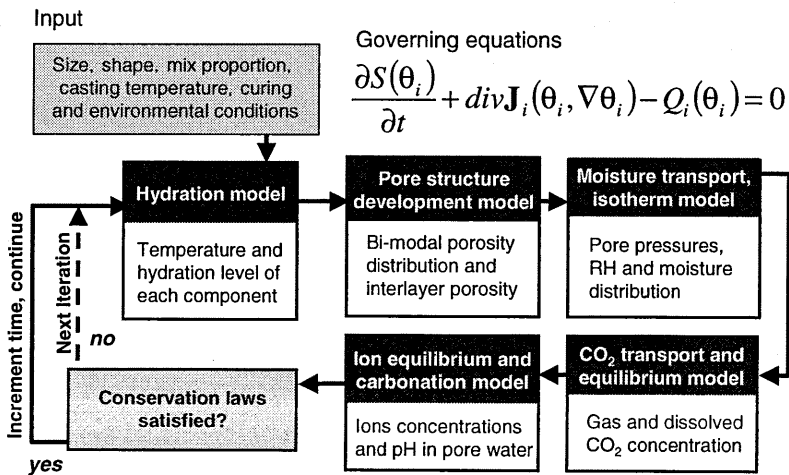


Fig.7 Overall framework of thermo-hygro system DuCOM

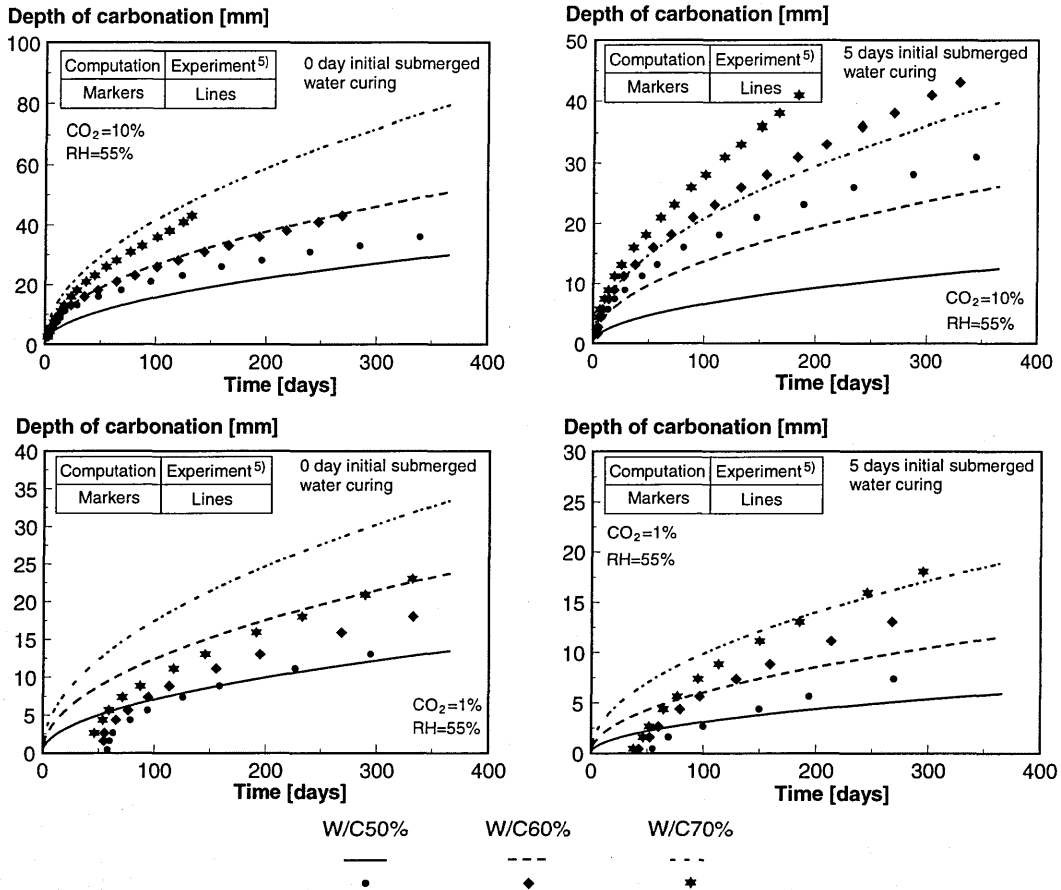
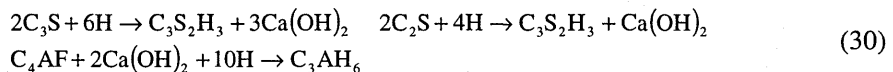


Fig.8 Prediction of carbonation phenomena for different CO₂ concentrations, W/C and curing conditions

As degrees of freedom, temperature T [K], pore pressure P [Pa], and dissolved carbon dioxide ρ_d [kg/m³] are solved in the system such that the mass/energy balance equations are fully satisfied (Fig.7). The inputs required in the scheme are mix proportion, powder material characteristics, casting temperature, geometry of the target structure, and the boundary conditions to which the structure will be exposed during its life-cycle. Regarding the boundary conditions, the input values of each degree of freedom are applied to the specified boundary nodes in the finite elements.

The amount of Ca(OH)₂ in cementitious materials can be obtained from the multi-component hydration model as [23][24],



When blast furnace slag and/or fly ash are mixed into concrete, Ca(OH)₂ is consumed during hydration due to the pozzolanic reaction. The consumption ratios of slag and fly ash reactions are assumed to be 22% and 100% of the reacted mass, respectively, in this analysis [23][24].

4.2 Verification with accelerated carbonation tests

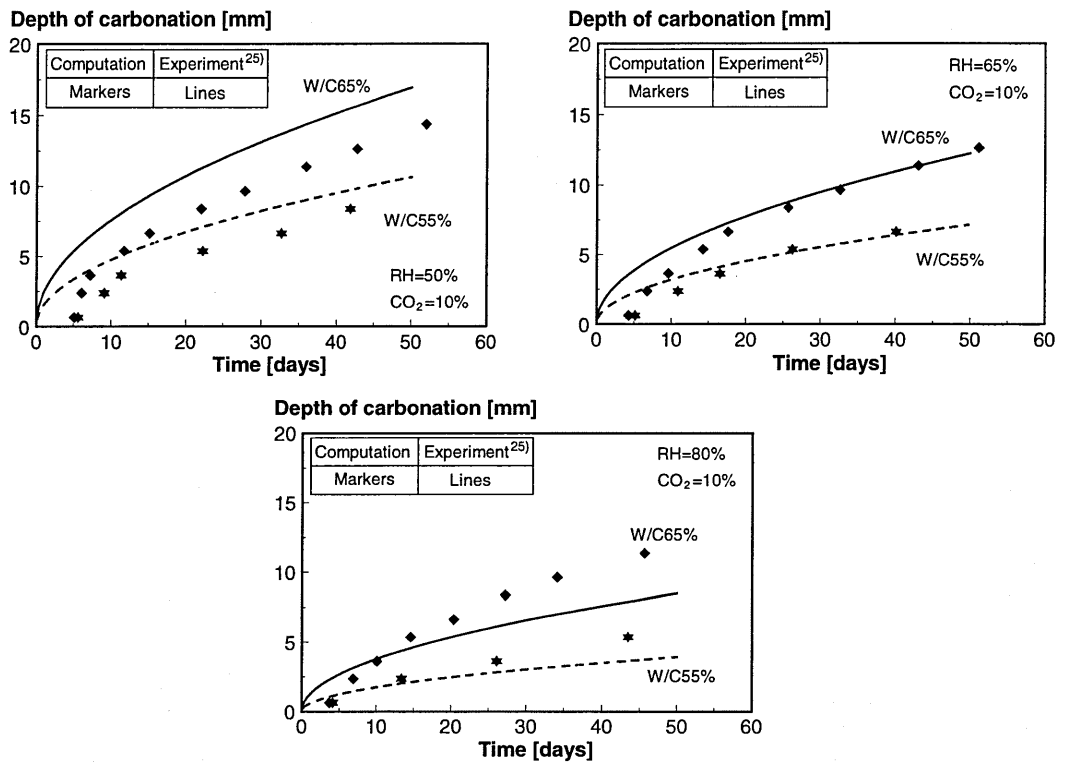


Fig.9 Prediction of carbonation phenomena for different W/C and ambient relative humidity

Firstly, accelerated carbonation tests were used for verification. Experimental data obtained by *Uomoto et al* were used for this purpose [6]. The data are for cylindrical specimens of radius 10cm and height 20cm. After two days of sealed curing, two curing conditions were specified: submerged in water for 0 days, and cured in water for five days. After the prescribed curing periods, specimens were kept in a controlled chamber where the concentrations of CO₂ gas (1.0% and 10%), temperature (20 °C), and relative humidity (55%RH) were kept constant. The water-to-cement ratios of the specimens were 50%, 60%, and 70%. The unit weight of water was held constant in the mix proportions. Results of the verifications are shown in Fig.8. All of the input values in the analysis corresponded to the experimental conditions. Analytical results show the relationship between exposure time and the concrete depth at which the pore water pH falls below 10.5, which is the phenolphthalein indicator point. The empirical formulae shown in the figures were regressed with the *square root t equation*. In the discussion in previous chapters, the equilibrium constants and the reaction rate coefficient in the modeling are assumed for a constant temperature of 25 °C. Therefore, strictly speaking, it is not correct to compare experimental results carried out at 20°C. However, it has been reported in the past that the difference in carbonation progress between 20°C and 25°C is a few percent only [25]. Considering the precision of the current models, we judge that sensitivity to temperature might not be large, so the parameters for 25°C were used in the analysis. The simulations are able to roughly predict the progress of carbonation for different CO₂ concentrations and water-to-powder ratios.

Next, the effect of ambient relative humidity on the progress of carbonation was verified using experimental data obtained by *Mihashi et al* [25]. After one day of wet curing, specimens were stripped, and then cured under standard curing conditions until the age of 28 days before being kept at 50%RH and 20°C for 10 days. In the accelerated test, specimens were exposed to a 10%

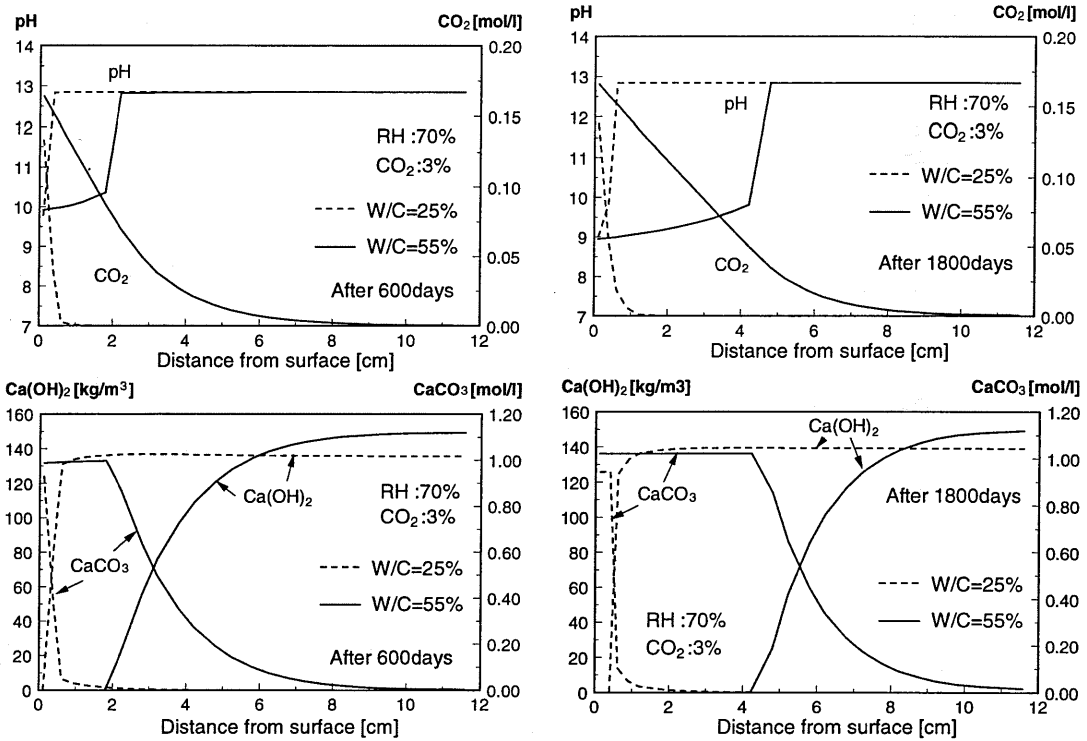


Fig.10 Distribution of pH, calcium hydroxide and calcium carbonate under the action of carbonic acid

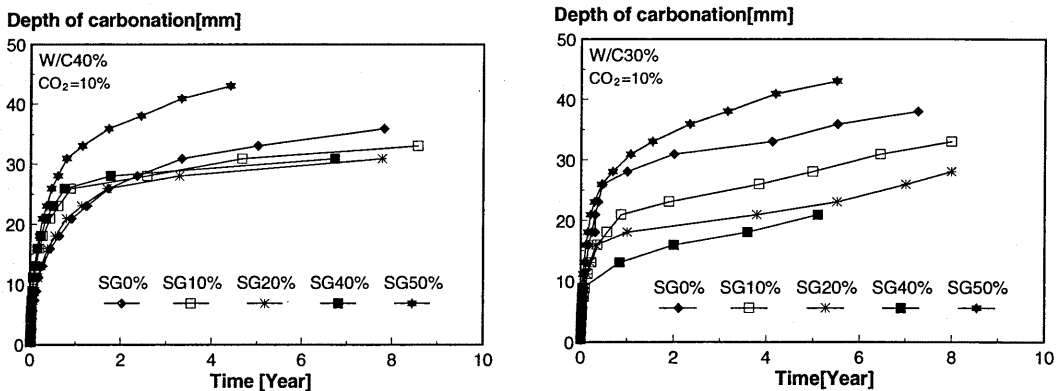


Fig.11 Effect of blast furnace slag on carbonation progress

concentration of CO₂ at a constant temperature of 25°C, and at three different ambient relative humidities: 50%RH, 65%RH, and 80%RH. Two cases of water-to-cement ratio were tested (W/C=65% and 55%). Figure 9 shows the results of the verification. The depth of carbonation for various ambient relative humidities can be predicted with reasonable accuracy by the proposed method.

4.3 Distribution of pH, calcium hydroxide, and calcium carbonate

Figure 10 shows the distribution of pore water pH, CO₂, calcium hydroxide, and calcium

carbonate within concrete exposed to a CO₂ concentration of 3%. Two different water-to-powder ratios, W/C=25% and 50%, were specified in the analysis, and these specimens were exposed to CO₂ gas after 7 days of sealed curing. Consumption of calcium hydroxide, formation of calcium carbonate, and reduction of pH with time are estimated by the analysis. It is also shown that a higher resistance to carbonic acid action is achieved in the case of low W/C.

4.4 Influence of admixtures on carbonation phenomenon

A sensitivity simulation was carried out to demonstrate the influence of admixtures on the carbonation phenomenon. Blast furnace slag was mixed into concrete at six different ratios to the total weight of powder (0%, 10%, 20%, 40%, and 50%). In this series, the water-to-powder ratio was specified as 30% and 40%. Numerical results are shown in Fig.11. In the case of W/P 30%, as the amount of slag increases, the carbonation rate decreases because a dense micro-pore structure is achieved. However, if 50% of the total powder is replaced with slag, the resistance to carbonation falls slightly, since the effect of Ca(OH)₂ consumption due to the pozzolanic reaction becomes significant. On the other hand, in the case of W/P 40%, the ratio of slag does not seem to influence the rate of carbonation in the range of 0%-40%. This arises from the influence of two factors; an increment in Ca(OH)₂ consumption and the dense micro-pore structure achieved by using slag.

5. Conclusions

For the purpose of establishing an evaluation method for the carbonation phenomenon, formulations are developed for the equilibrium of gaseous and dissolved carbon dioxide, their transport, ionic equilibria, and the carbonation reaction process. The main feature of this work is that the model is based on micro-physical phenomena, enabling the pH profile of pore water and degradation of the micropore structure to be predicted for arbitrary conditions. This contrasts with the conventional approach, where depth of carbonation is generally evaluated using an empirical formula. By means of the proposed methodology, it is possible to predict not only the carbonation phenomenon, but also the pH profile in pore solutions attacked by other acids, such as sulphuric acid, and nitric acid. Through various numerical simulations, it is shown that the proposed modeling technique can roughly predict carbonation progress and pH fluctuations for different mix proportions, curing conditions, and environmental conditions.

References

- [1] JCI: *The report of JCI Committee on Carbonation*, 1993.
- [2] Sakai, E.: Carbonation reaction, *Cement chemistry*, pp.105-112, Japan Cement Association, 1993.
- [3] Hamada, M.: Concrete carbonation and steel corrosion, *Cement/Concrete*, No.272, pp.2-18, 1969.
- [4] Kishitani, K.: *Durability of reinforced concrete*, pp.165, 1963.
- [5] Nagataki, S., Ohga, H. and Saeki, T.: Analytical prediction of carbonation depth, *Annual report of cement technology*, No.41, pp.343-346, 1987.
- [6] Uomoto, T. and Takada, Y.: Factors Affecting Concrete Carbonation Ratio, *Concrete Library of JSCE*, No.21, pp.31-44, 1993.
- [7] Saeki, T., Ohga, H. and Nagataki, S.: Mechanism of Carbonation and Prediction of Carbonation Process of Concrete, *Concrete Library of JSCE*, No.17, pp.23-36, 1991.
- [8] Papadakis, V.G., Vayenas, C.G. and Fardis, M.N.: Fundamental modeling and experimental investigation of concrete carbonation, *ACI Material Journal*, pp.363-373, Vol.88, No.4, 1991.
- [9] Saetta, A.V., Schrefler, B.A., and Vitaliani, R.V.: The carbonation of concrete and the mechanisms of moisture, heat and carbon dioxide flow through porous materials, *Cement and Concrete Research*, Vol.23, pp.761-772, 1993.
- [10] Saetta, A.V., Schrefler, B.A., and Vitaliani, R.V.: 2-D model for carbonation and moisture/heat flow in porous materials, *Cement and Concrete Research*, Vol.25,

pp.1703-1712, 1995.

- [11] Osada, M., Ueki, H., Yamasaki, T. and Murakami, M.: Simulation analysis on carbonation reaction of concrete members taking alkali element into consideration, *Proceedings of JCI*, Vol.19, No.1, pp.793-798, 1997.
- [12] Matsumoto, Y., Ueki, H., Yamasaki, T. and Murakami, M.: Model analysis on carbonation reaction with redissolution of CaCO_3 , *Proceedings of JCI*, Vol.20, No.2, pp.961-966, 1998.
- [13] Maekawa, K., Kishi, T. and Chaube, R. P.: *Modelling of Concrete Performance*, E&FN SPON, 1999.
- [14] Cusack, N. E.: *The Physics of Structurally Disordered Matter*, Bristol edition, 1987.
- [15] Welty, J.R., Wicks, C.E., and Wilson, R.E.: *Fundamentals of momentum, heat, and mass transfer*, John Wiley & Sons, Inc., 1969.
- [16] Kunii, T. and Hurasaki, S.: *The Theory on Transfer Rate*, Bai-hu Kan press, 1980.
- [17] Kobayashi, K., Syutto, K.: Diffusivity of oxygen in cementitious materials, *Concrete Engineering*, Vol.24, No.12, pp.91-106, 1986.
- [18] Papadakis, V.G., Vayenas, C.G. and Fardis, M.N. : Physical and chemical characteristics affecting the durability of concrete, *ACI Material Journal*, pp.186-196, Vol.88, No.2, 1991.
- [19] Kobayashi, K.: Carbonation of concrete, *Proceedings of JSCE*, No.433/V-15, pp.1-14, 1991.
- [20] Freiser, H. and Fernando, Q.: *Ionic Equilibria in Analytical Chemistry*, John Wiley & Sons, Inc., 1963.
- [21] Ishida, T., Chaube, R.P., Kishi, T. and Maekawa, K.: Modeling of pore water content in concrete under generic drying wetting conditions, *Concrete Library of JSCE*, No.31, pp.275-287, 1998.
- [22] Ishida, T. and Maekawa, K.: An integrated computational system for mass/energy generation, transport, and mechanics of materials and structures, *Concrete Library of JSCE*, No.36, pp.129-144, 2000.
- [23] Kishi, T. and Maekawa, K.: Multi-component model for hydration heating of Portland cement, *Concrete Library of JSCE*, No.28, pp. 97-115, 1996.
- [24] Kishi, T. and Maekawa, K.: Multi-component model for hydration heating of blended cement with blast furnace slag and fly ash, *Concrete Library of JSCE*, No.30, pp. 125-139, 1997.
- [25] John, J., Hirai, K. and Mihashi, H.: Influence of environmental moisture and temperature on carbonation of mortar, *Concrete Research and Technology*, Japan Concrete Institute, Vol.1, No.1, pp.85-94, 1990.
- [26] Tanano, H. and Masuda, Y.: Mathematical model on progress of carbonation of concrete, *Proceedings of JCI*, Vol.13, No1, pp.621-622, 1991.